Assessing the functional groups in activated carbons through a multi-technique approach

Assessing the functional groups in activated carbons through a multi-technique approach

Eleonora Vottero,[a,b] Michele Carosso,[a] Riccardo Pellegrini,[c] Andrea Piovano,[b,*] Elena Groppo[a,*]

a. Department of Chemistry, NIS Centre and INSTM, University of Turin, Via G. Quarello 15/A, Turin, I-10135, Italy.
b. Institut Laue-Langevin (ILL), 71 Avenue des Martyrs, 38042 Grenoble, France.
c. Chimet SpA–Catalyst Division, Via di Pescaiola 74, Viciomaggio Arezzo, I-52041, Italy.

Abstract

Activated carbons play a key role in catalytic applications thanks to the possibility to tune their surface chemistry through the change of the precursor or of the activation treatment. However, the characterization of their surface species is not straightforward. Herein, we present the potentials of a multi-technique approach, based on an alternative Temperature Programmed Desorption - Infrared (TPD-IR) method coupled with TGA, elemental analysis and Boehm titration measurements, for the simultaneous identification and quantification of functional groups in activated carbons. We employed this method for characterizing seven carbons used in catalysis, differing in precursors, activation routes and post-activation treatments. The novelty of our TPD-IR approach relies in the choice of accumulating the gaseous decomposition products while maintaining the necessary low-pressure levels. The univocal detection of released gases by IR spectroscopy permits the quantification of those released at high concentration (CO_2 and CO) as well as those produced at trace levels (e.g. CH_4, NO). Moreover, H_2O may be quantified, giving information on the fraction of functional groups close enough to condense. Even though this type of characterisation remains a challenging task, our alternative TPD-IR approach appears as a promising and versatile new option to identify and quantify the surface functional groups on different carbon materials, which hopefully will benefit of a wider and more thorough validation by independent research groups in the near future.

1. Introduction

Activated carbons are high surface area materials, employed in applications ranging from adsorption, storage, environmental remediation, catalysis and many others.[1-7] They are obtained from different carbonaceous precursors (wood, peat, coconut shells, etc.) following either a physical or a chemical activation route.[4-5] In the former case, the precursor is carbonized at high temperature in inert atmosphere and then activated by weakly reactive species such as steam or CO_2, while in the latter case the precursor is impregnated by a chemical agent (such as $ZnCl_2$ or H_3PO_4) prior carbonization. They can be further modified by post-activation treatments,[8-11] for example by strong oxidizing agents. Both the precursor and the activation route affect the textural properties (e.g. specific surface area and porosity),[12-13] as well as the concentration of heteroatoms and the nature and content of the functional groups determining their chemical properties.[14-16] Identifying and quantifying the functional groups in an activated carbon is particularly important since they play a relevant role in most of their applications. For example, electronegative heteroatoms modify the polarity of the carbon surface, with consequences on its adsorption, wettability and reactivity properties.[1, 17] Functional groups can also generate specific interactions with other molecules, which can be favourable or detrimental to specific applications.[18] In catalysis, the presence of surface functionalities is relevant for providing a high dispersion and stability of the metallic phases or even for anchoring the metallic phases as coordination complexes.[19]

Many experimental techniques allow, in principle, a direct characterization of the functional groups in activated carbons. For example, the Boehm titration method[20-21] allows the quantification of the O-containing functional groups displaying acidic or basic properties, but it cannot account for neutral species. X-ray photoelectron spectroscopy (XPS) permits to perform a semi-quantitative analysis of some O-containing functional groups,[22] but it suffers of some drawbacks:[16, 23-24] i) it may lead to misleading results for microporous carbons (since photoelectrons preferentially probe the external surface, which is usually more oxidized than the internal one); ii) the unequivocal quantification of specific O-containing groups is quite subjective; iii) some groups are undistinguishable, while others (e.g. lactones) contribute simultaneously at two different peaks in the spectrum. Infrared spectroscopy (mostly performed in DRIFT mode) allows in principle the detection of all the IR active functional groups,[18, 25-26] but the bands assignment is often challenging, and even more so is the quantification of the species. Inelastic neutron scattering spectroscopy is useful to detect H containing species,[26-28] but is poorly sensible to other elements such as O or N. Raman spectroscopy provides information on the degree of aromaticity and disorder of C-C bonds in the graphitic platelets,[29] but is weakly sensible to peripheral species.

To overcome these limitations, TPD (Temperature Programmed Desorption), which demonstrated to be a solid approach for the identification and quantification of adsorbed species,[30-33] has been traditionally used to indirectly identify and quantify functional groups in activated carbons.[8-9, 34-44] In such case, the technique exploits the fact that each functional group decomposes within a specific temperature range, generating a few gaseous molecules that, for O-containing functional groups, usually consist in CO, CO_2 and H_2O. Extended studies in the literature allow estimating the decomposition products and the decomposition temperature for the main O-containing functional groups, as summarized in Figure 1. The characteristic temperature intervals for the decomposition of each functional group span over large ranges because of their intrinsic

heterogeneity, but also because TPD spectra are affected by the type of carbon and the way the TPD experiments are carried out. Nevertheless, some general trends can be readily noticed: 1) the low temperature range (T < 400 °C) is generally attributed to the decomposition of carboxylic acid groups to CO_2;[36-37, 45] 2) the intermediate temperature range (400 °C < T < 560 °C) is characteristic for the decomposition of carboxylic anhydrides to CO_2 + CO and of a fraction of lactones to CO_2;[36-37, 45-46] 3) in the high temperature range (T > 560 °C), beside the remaining lactones which decompose to CO_2, phenols, ethers, carbonyls and quinones decompose to CO.[36-37, 45-46]

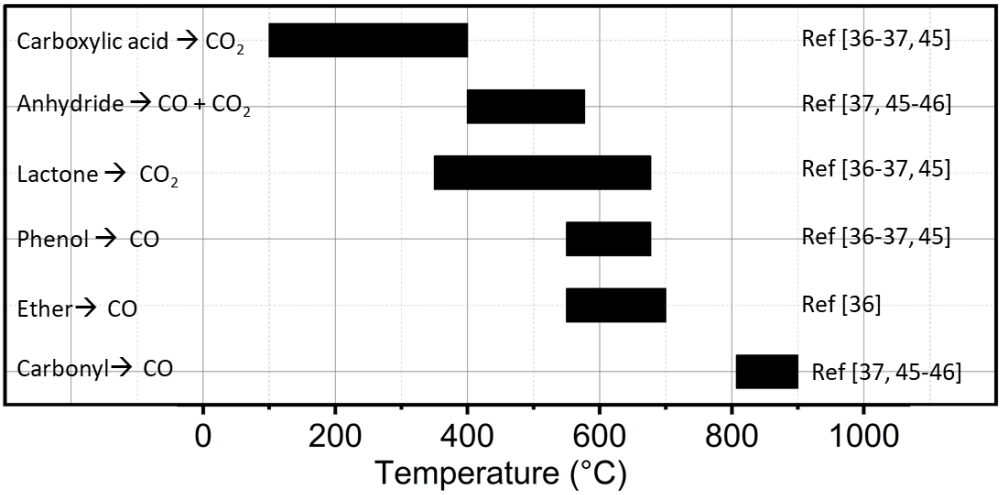

Figure 1: Decomposition temperature intervals for the main oxygen containing functional groups as reported in the literature.

Most of the studies in the literature focus on the formation of CO and CO_2, but the release of H_2O is also observed, although rarely discussed. Weakly adsorbed water gives origin to a large TPD peak at T < 200 °C,[8, 47] unless this fraction is removed from the samples before the TPD experiment by a treatment in vacuum, in an inert gas flow and/or modest heating (T < 150 °C). Some works[8, 47-48] pointed out the presence of H_2O peaks in the TPD runs at higher temperatures, which were attributed either to the desorption of strongly adsorbed water hydrogen-bonded to oxygen-containing functional groups (T < 400 °C) or to the condensation of two adjacent functional groups with the removal of a H_2O molecule (for example, two carboxylic acids may condense to form an anhydride, or a carboxylic acid and a phenol may condense to form a lactone, or two phenols may condense to give an ether). The evolution of H_2O at temperature higher than 200 °C was also interpreted as due to the direct decomposition of some functional groups. In particular, Li et al.[49] ascribed the simultaneous evolution of CO and H_2O at ca. 240 and 330 °C to the decomposition of carboxylic acids groups through an alternative route. Vivo-Vilches et al.[50] instead reported the contemporary evolution of CO, CO_2 and H_2O at ca. 280 °C, attributing these products to the formation and immediate decomposition of an anhydride group from two adjacent carboxylic acid groups. In this perspective, also part of the H_2O released during a TPD run should be accounted for the total O content in an activated carbon.

During a typical TPD experiment on an activated carbon, the sample is heated under an inert gas flow and the decomposition products are detected and quantified on-line by gas chromatography (GC), mass spectrometry (MS) or infrared (FT-IR) spectroscopy.[42, 51-52] The

drawback of this approach is that some species may escape on-line detection and the sensitivity for quantitative analysis is not so high, so that this approach cannot be applied to carbons with a very small amount of surface oxygen groups. In a few cases, and in particular for graphite based samples, the TPD experiments have been conducted under dynamic vacuum or very low pressure values and the measurement of the released gases was performed by MS.[42-44, 53-55] Recently, Ishii et al.[42] developed a TPD apparatus consisting of a quartz reactor and a high vacuum detecting unit equipped with a quadrupole mass spectrometer, with which they have been able to quantify the amount of CO, CO_2 and H_2O with a sensitivity of about 0.1 pmol/s.

In this work, we developed an alternative experimental approach to perform a systematic TPD study on several activated carbons: we worked in static conditions, accumulating low-pressure levels of the gaseous products in a known volume, and used FT-IR spectroscopy for their detection and quantification. The large temperature gradient between the heated sample and the IR measuring cell is the driving force to desorb the gaseous products, which preferentially migrate from the former to the latter. The accumulation of low amount of decomposition products in the IR cell as an alternative to gas flux allowed us to detect and often quantify minor decomposition products otherwise not visible. Important advantages of our approach are the following: 1) the experimental set-up is very simple and achievable by standard equipment in the lab; 2) our system is also flexible regarding the amount of sample, allowing to measure with good resolution the TPD profile of carbons containing either low or high concentration of functional groups; 3) the identification of the produced gases by FT-IR spectroscopy is straightforward, because the IR roto-vibrational profile of each gas is univocal; 4) their quantification is simply possible exploiting the Lambert-Beer law, after a careful but simple calibration. The most important drawback so far is the maximum temperature achievable (700 °C) with our setup, which does not allow to quantify in a direct way the more thermostable functional groups.

We combined this TPD-IR approach with elemental analysis (EA), thermogravimetric analysis (TGA) and Boehm titration (BT) to characterize seven activated carbons used in catalysis, produced from different precursors and following different activation routes and post-activation treatments. These samples are highly pure and similar in terms of morphology and textural properties, but different from the point of view of surface chemistry. Therefore, the information obtained with the various techniques is directly comparable without further assumptions. Moreover, CwA, CwA-ox, Cchemi and Cchemi-ox samples were already extensively characterized by our research group in the past employing a large variety of techniques among which N_2 adsorption, SEM, XRPD, DRIFT, Raman, INS, XPS, ^{13}C and ^{1}H NMR,[18, 26-28] but never performing a systematic identification and quantification of the main functional groups. The results obtained on this set of carbons offered us the possibility to critically compare the advantages/disadvantages of various methods in the identification and quantification of surface functional groups in carbon-based materials.

2. Experimental

2.1 Samples

All the activated carbons examined in the present work were provided by Chimet S.p.A.[56] Four of the carbons were physically activated by steam, two of them originating from wood (CwA and CwB) and two from peat (CpA and CpB). Cchemi was obtained via a chemical activation procedure by means of H_3PO_4 on a wood precursor. All the carbons contain a minor amount of ashes, slightly higher for carbons of peat origin than for those of wood origin (0.58, 0.38, 5.51, 2.96 and 1.96 wt% for CwA, CwB, CpA, CpB and Cchemi, respectively, as quantitatively determined by calcination). Compositional analysis indicates that they are mainly composed of silicoaluminates. Finally, CwA-Ox and Cchemi-Ox were obtained from CwA and Cchemi, respectively, by a post-activation treatment in concentrated HNO_3 (67% w/w) at room temperature for 24 h, followed by washing steps in distilled water until reaching neutral pH. The amount of ashes after treatment in HNO_3 was found to be negligible.

2.2 Textural characterization and evaluation of physisorbed water

The surface area and pore volume of the carbons were determined by N_2 physisorption measurements at 77 K. Measurements were performed on a Micromeritics ASAP 2020 instrument. The adsorption isotherms were analysed according to the procedure described in[57]. All the carbons were subjected to systematic TGA measurements in the 30 – 120 °C temperature interval to quantify the amount of physisorbed water, The measurements were performed with a Q600 SDT TA instrument, in N_2 flux (100 ml/min) and with a heating ramp of 5 °C/min.

2.3 Composition

CHNS elemental analysis (EA) was carried out with a Thermo Fisher Scientific FlashEA 1112 Elemental Analyzer. 2,5-bis(5-tert-butyl-benzoxazol-2-yl)thiophene (BBOT) was used as standard for calibration. About 1.7- 2.0 mg of sample has been used for each measurement, as a compromise in the quantification of C vs. H, N and S. The samples were loaded together with some V_2O_5 catalyst into tin capsules and then measured, three repetitions were performed and the results averaged. Each measurement was separated from the successive one by a by-pass empty run only containing the V_2O_5 catalyst to clean the setup and to avoid artifacts.

2.4 Boehm titration

All the carbons were titrated with NaOH, Na_2CO_3 and $NaHCO_3$, following the indication by Boehm.[21] 0.3 grams of each carbon were placed in separate plastic bottles, and then 25 ml of 0.05 M NaOH, Na_2CO_3 and $NaHCO_3$ solution were added. After gently shaken for 48 hours, the solutions were filtrated. The amount of base adsorbed by each carbon was determined by back titration of the solution with a standardized HCl solution.

2.5 TPD-IR measurements

2.5.1 Set-up and experimental protocol

A simplified scheme of the experimental setup developed in this work for the TPD-IR measurements is reported in Figure 2A. It consists of a quartz tube to host the activated carbon (a), an oven (b), an

IR cell especially designed for the detection of gases (optical path of 17 cm, c) which is inserted within a FT-IR spectrophotometer (c'), a valve to isolate the system (d) and a vacuum line (e). All the parts are connected through small diameter plastic tubes via Swagelok connections to ensure flexibility to the entire system, short enough to avoid water condensation. The whole apparatus is extremely simple and achievable by standard lab equipment, provided that an IR spectrophotometer is available. The only drawback is that, currently, the thermal resistance of some parts of the set-up does not allow us to exceed the heating temperature of 700 °C.

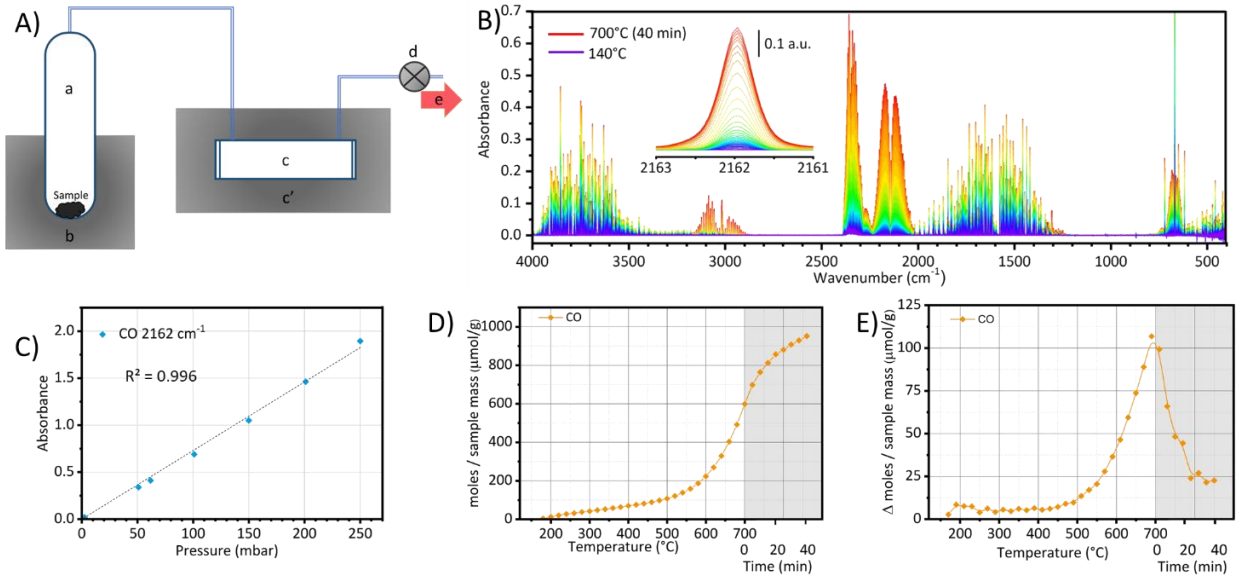

Figure 2: Part A): Schematic representation of the experimental set-up developed in this work for the TPD-IR measurements: a) quartz tube; b) oven; c) IR cell for the detection of gases; c') FT-IR spectrophotometer; d) valve; e) vacuum line. Part B): Example of the raw FT-IR spectra as collected during a TPD run. Part C): calibration line for CO, which correlates the absorbance of the peak at 2162 cm^{-1} (magnified in the inset of Part B) to the corresponding equilibrium pressure (in mbar). Part D): Cumulative moles plot for CO, as determined from the analysis of the raw IR spectra reported in part B), applying the calibration line shown in part C after the temperature correction described in the Supporting Information, Section S2. Part E): Differential moles plot for CO, where each point is the number of moles of gas released by the carbon between the collection of two consecutive FT-IR spectra. In parts D and E, the temperature ramp range is reported in white background, while the isotherm range in grey background.

In a standard experiment, the activated carbon is inserted in the quartz tube. The mass varied between ca. 0.2 and 0.8 g, depending on the estimated concentration of functional groups. The tube is connected to the IR cell and the IR cell to the vacuum line, and the whole system is evacuated. Subsequently, the tube is inserted in the oven, a thermocouple is placed close to the sample, and the activated carbon is heated at 120 °C overnight in dynamic vacuum, in order to remove the weakly physisorbed water. This step allows also for the cleaning from moisture of the whole apparatus. An IR background is then collected, and the TPD run is started. Valve D is closed and the sample is heated at 5 °C/min up to 700 °C, followed by an isotherm at the same temperature for 40 minutes. During the whole TPD run the produced gases are accumulated in the system volume, and FT-IR spectra are collected every 20 °C (i.e. 4 minutes) during the ramp, and every 5 minutes during the isotherm. The FT-IR spectra were collected with a Nicolet 6700 instrument

equipped with a MCT detector, averaging 32 scans, and at a resolution of 0.5 cm^{-1} in order to resolve the roto-vibrational profile and to identify gases present in very low concentrations.

Even though our set-up is based on the accumulation of the produced gases, the large temperature gradient between the heated sample and the IR measuring cell guarantees the fast migration of the desorbed products from the sample to the IR cell. This effect is supported by a blank experiment where we heated known amount of CO or CO_2 within the same set-up without the sample: the intensity of the IR spectra increased as a function of temperature, denoting that the gases rapidly diffuse toward the IR cell. This avoids the accumulation of the products inside the sample, minimizing the occurrence of secondary reactions (vide infra section 3.2.1).

2.5.2 Data elaboration

A typical outcome of a TPD-IR run is reported in Figure 2B. Each IR spectrum detects simultaneously all the gases released at a certain temperature. Since the experiment consists in the accumulation of the gases within the IR cell, a progressive increase of the intensity of the overall IR spectra is observed. It is worth noticing that with this set-up we worked in the optimal absorbance range that allowed acquiring high-resolution spectra, most appropriate for a quantitative FT-IR analysis. In order to quantify the partial pressure of a certain gas at each IR spectrum, calibration lines were obtained by measuring the IR spectra of known pressures of the pure gas. Knowing the volume of the whole set-up, the moles of gas in correspondence with each spectrum can be calculated by employing the perfect gas law. Calibration lines for CO, CO_2, H_2O, CH_4 and NO were measured: Figure 2C shows as an example the calibration line for CO, while the others are reported in Figure S1 in the Supporting Information. The quantification of SO_2 was performed by using the molar extinction coefficient value of 0.0103 $(\mu mol/mol)^{-1}m^{-1}$ at 1374.04 cm^{-1} as reported in the NIST database.[58-59]

A further correction accounting for the effects of an uneven temperature distribution among different sections of the set-up was necessary for a correct quantitative analysis, as discussed in Section S2. The so corrected absorbances were used to calculate the corresponding gas partial pressures, and from the pressures the number of moles present in the IR cell at each temperature (cumulative moles plot, Figure 2D). In order to better visualize the production rate of the gases at each temperature, difference plots were finally obtained, as reported in Figure 2E, where each point represents the number of moles of gas released by the carbon between the collection of two consecutive FT-IR spectra. These plots are perfectly comparable with those obtained with conventional TPD apparata, as reported in the literature.[8-9, 34-44] The points collected during the temperature ramp from 120 to 700 °C are shown on white background, while those collected during the 40 min isotherm run at 700 °C on grey background.

2.5.3 Evaluation of the relevance of secondary reactions on the TPD results

The possibility of secondary reactions between the gaseous decomposition products and the functional groups still present in the carbon pores is reported in the literature.[39, 43, 60] These reactions may alter the ratios among the decomposition products and cause erroneous assignment. Secondary reactions have been reported to occur especially on higher oxidized carbons inside micropores, where the residence time of the decomposition products is long enough to favour the reaction with an oxygen-containing functional group before diffusing out of the pore. For the same

reasons, it has been demonstrated that secondary reactions play a major role at atmospheric pressure, while they become negligible under reduced pressure (below 30 mbar) or in vacuum.[39, 43, 60] Since our experimental set-up works at reduced pressures we did not expect that secondary reactions will have a relevance on our results. Nevertheless, to definitely exclude them, a series of tests as suggested in the literature have been performed on the carbon characterized by the largest amount of functional groups, namely Cchemi-Ox. The results are showed in Figure S3 and summarised in the following.

1. One of the best way to diminish the secondary reaction is to perform the TPD experiment under vacuum or very reduced pressure;[39, 43, 60] therefore, we repeated the TPD run with ten times less sample, so that the maximum pressure in the whole system remained well below 30 mbar (Figure S3A).
2. It is also recommended to change the heating rate:[36, 60] as the total amount of CO_2 varies as a function of the heating rate only in the case of secondary reactions. Hence, the TPD experiment was repeated at a heating rate of 15°C/min (Figure S3B).
3. Finally, it has been suggested that when CO (or CO_2) are pre-adsorbed on the carbon just before the TPD run, [39, 43, 60] larger CO_2 (or CO) desorption than those measured without pre-adsorption indicate secondary reactions. Therefore, we performed two additional experiments as follows. Cchemi-Ox was placed in the quartz tube and degassed in dynamic vacuum at 120 °C overnight. Then, about 400 mbar of the pre-adsorbing gas (CO or CO_2) was introduced in the reactor and left in contact with Cchemi-ox at 120 °C for 2 hours. After that, the system was rapidly degassed until reaching a pressure lower than 1 mbar and the TPD experiment was started (Figure S3C and D).

The differential TPD spectra of CO and CO_2 with ten times less sample (Figure S3A) and at a heating rate of 15 °C/min (Figure S3B) were very similar to the reference one (with a maximum 1% difference which is considered the level of precision of our measurements). The pre-adsorbed gases CO and CO_2 are mainly desorbed along the experiment (Figure S3C and D), while their conversion to CO_2 or CO appears very limited, analogously to other results reported in literature and considered negligible.[39] All in all, these data imply that, in our experimental conditions, secondary reactions can be considered negligible and hence the TPD data are representative of the true nature of carbon surfaces.

2.6 TGA measurements up to 1000 °C

Additional TGA measurements were performed on Cchemi and CwA-ox up to 1000 °C under inert gas flow (N_2, 100 ml/min) with a Q600 SDT TA instrument. The TGA measurements were designed to follow the most similar experimental protocol to the TPD-IR experiments as possible. Thus, after being charged in the TA instrument, the sample was kept for at least 3 h under N_2 flux at 120°C to remove the physisorbed H_2O, and then the sample was heated up to 1000 °C with a 5 °C/min temperature ramp.

3. Results and Discussion

3.1 Texture and composition

Table 1 reports for all the carbons: the values of specific surface area (SSA_{BET}) and micropore volume (V_{micro}) as determined by N_2 physisorption measurements; the amount of physisorbed water obtained from TGA measurements; the C, H, N and S composition determined by elemental analysis (CHNS analysis), and that of O obtained by difference. The textural properties of the most of the carbons were discussed in our previous work.[18] For sake of completeness, the N_2 adsorption isotherms are reported in Figure S4. Interestingly, the TGA data indicate that the amount of physisorbed water is not related to the textural properties (Figure S5). For example, CwB has the same V_{micro} than CwA, but contains the double of physisorbed water; or CwB and CpB display a sensibly different SSA_{BET}, but contain the same amount of water.

Table 1: Textural and compositional properties of the activated carbons analysed in the present work: specific surface area (SSA_{BET}) and micropore volume (V_{micro}) as determined by N_2 physisorption measurements; amount of physisorbed water obtained by TGA measurements (H_2O-physi); C, H, N and S composition as obtained by elemental analysis, and that of O obtained by difference.

Carbon	SSA_{BET} (m^2/g)	V_{micro} (cm^3/g)	H_2O-physi (Δw/w%)	C (w/w%)	H (w/w%)	N (w/w%)	S (w/w%)	O (w/w%)
CwA	1018	0.63	2.9	91.9 ± 0.5	0.50 ± 0.02	0.30 ± 0.04	-	7.3 ± 0.6
CwB	1325	0.65	5.9	88.3 ± 3.2	0.32 ± 0.03	0.29 ± 0.03	-	11.1 ± 3.2
CpA	903	0.49	8.7	81.7 ± 0.6	0.15 ± 0.01	0.41 ± 0.03	0.10 ± 0.01	17.7 ± 0.7
CpB	882	0.52	5.7	86.2 ±1.9	0.26 ± 0.03	0.44 ± 0.03	-	13.1 ± 1.9
Cchemi	1508	1.11	4.8	83.6 ± 1.6	1.43 ± 0.10	0.20 ± 0.04	-	14.8 ± 1.7
CwA-ox	949	0.59	10.6	76.5 ± 1.9	0.52 ± 0.05	1.02 ± 0.06	-	21.9 ± 2.1
Cchemi-ox	1442	1.13	14.6	64.0 ± 1.3	0.87 ± 0.04	2.44 ± 0.06	-	32.7 ± 1.4

As far as the chemical composition is concerned, CHNS elemental analysis determines the absolute amounts of the elements carbon, hydrogen, nitrogen and sulphur. The difference to the total weight gives an estimation of the amount of oxygen, under the assumptions that the sample does not contain other elements. Subtle differences in composition are observed between the carbons. All activated carbons contain small amount of nitrogen. Carbons of peat origin contain more oxygen than those of wood origin, but less hydrogen. CChemi is the carbon with the highest H/C ratio, which suggests that it is that with the smallest graphitic domains (i.e. larger amount of H terminations), in agreement with our previous measurements.[26] Oxidation in nitric acid causes an increase in the amount of both nitrogen and oxygen, higher for CChemi-ox than for CwA-ox. Finally, sulphur is detected only in CpA.

3. 2 Boehm titration

The results of Boehm titration are summarized in Table 2. By using NaOH, Na_2CO_3 and $NaHCO_3$ different types of surface groups can be detected.[20-21, 61] $NaHCO_3$, which is the weakest base, titrates only the carboxylic acids and the anhydrides (which hydrolyses into two carboxylic acids). Na_2CO_3 titrates also lactones, while NaOH, which is the strongest base, titrates also phenols. Hence, Boehm titration allows to quantify lactones and phenols, while it does not discriminate between carboxylic acids and anhydrides. Interestingly, the results obtained by using NaOH and Na_2CO_3 as titrating

solutions are very similar in all the cases, which may lead to the conclusions that phenols are absent or negligible in all the carbons. However, it should be noticed that Boehm titration analyses the samples by chemical reactions in aqueous solutions, and this can influence the accessibility of the surface groups significantly (vide infra Section 3.6). As for the other functional groups, carbons of wood origin contain more carboxylic acids that lactones, while those of peat origin and Cchemi contain approximately the same amount of the two groups. Oxidation by HNO_3 causes a drastic increase of both surface species.

Table 2: Quantification of the acid functional groups by Boehm titration. The meq g^{-1} of each base reacted with the carbon are reported, as well as the amount of carboxylic acid + anhydrides, and lactones and phenols as difference.

Carbon	Acidity ($NaHCO_3$) (meq g^{-1})	Acidity (Na_2CO_3) (meq g^{-1})	Acidity (NaOH) (meq g^{-1})	carbox. acids + 2 anhydrides (meq g^{-1})	lactones (meq g^{-1})	phenols (meq g^{-1})[a]
CwA	0.19	0.21	0.20	0.19 ± 0.01	0.0± 0.1	0.0± 0.1
CwB	0.22	0.33	0.42	0.22 ± 0.01	0.1± 0.1	0.1± 0.1
CpA	0.16	0.32	0.32	0.16± 0.01	0.2± 0.1	0.0± 0.1
CpB	0.15	0.29	0.22	0.15± 0.01	0.1± 0.1	-0.1± 0.1
Cchemi	0.3	0.61	0.59	0.3± 0.01	0.3± 0.1	0.0± 0.1
CwA_ox	0.73	1.15	1.11	0.73± 0.01	0.4± 0.1	0.0± 0.1
Cchemi-ox	1.08	1.80	1.72	1.08± 0.01	0.7± 0.1	-0.1± 0.1

3.3 TPD-IR: gases observed and quantified by FT-IR spectroscopy at the end of the runs

Our TPD-IR approach allowed us to obtain a large number of details about each activated carbon. First of all, a careful inspection of the FT-IR spectra collected during the temperature ramp allowed us identifying all the gaseous products, including those produced in traces, as well as the exact temperature interval in which they are released. The FT-IR spectra collected at the end of each experiment contain the fingerprints of all the gases released by a given carbon during the TPD run, and are reported in Figure 3 (for CwA, CwB, CpA and CpB) and Figure 4 (for Cchemi, CwA-ox and Cchemi-ox), where the absorbance values were also normalized to the sample mass for a better comparison among the samples. In all the cases, the main decomposition products are CO, CO_2 and H_2O, but the analysis of the IR spectra revealed also the presence of other gases. In particular: i) CH_4 is observed in traces for CwA and CpB, while it is quantifiable for Cchemi; ii) SO_2 (bands at 1361, 1150 and 518 cm^{-1}) is clearly observed and quantifiable in the 400-600 °C interval for CwB, CpA and CpB. As for its origin, both wood and peat precursors are known for containing variable amounts of S;[62] iii) a quantifiable amount of NO, and other nitrogen containing molecules (NO_2 1615 cm^{-1}, N_2O 2223 and 1285 cm^{-1}, and HCN 3310 cm^{-1}) are observed in the IR spectra collected during the TPD run on the two oxidized carbons.

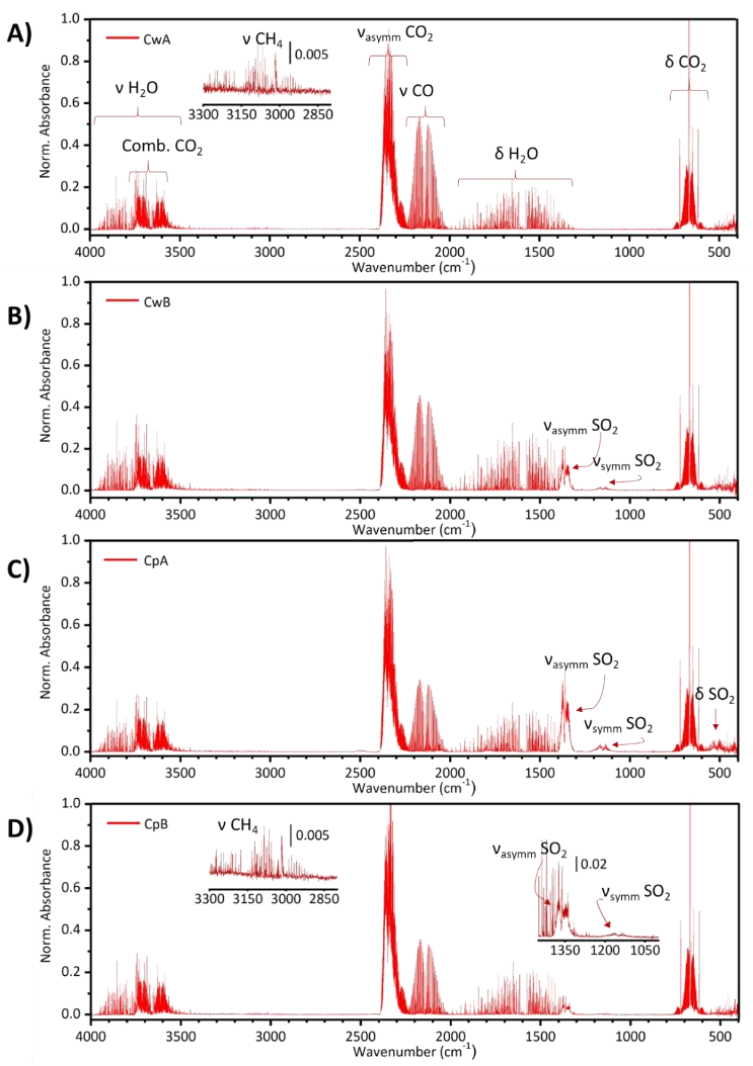

Figure 3: FT-IR spectra collected at the end of the TPD runs on CwA (part A), CwB (part B), CpA (part C) and CpB (part D). The absorbance values are normalized to the sample mass. The fingerprints of CO, CO_2 and H_2O, which are present in all the spectra, are indicated in part A. The fingerprints of the other compounds are indicated in the spectra when present, and in case of weak signals a magnification of that region of the spectra is reported as an inset.

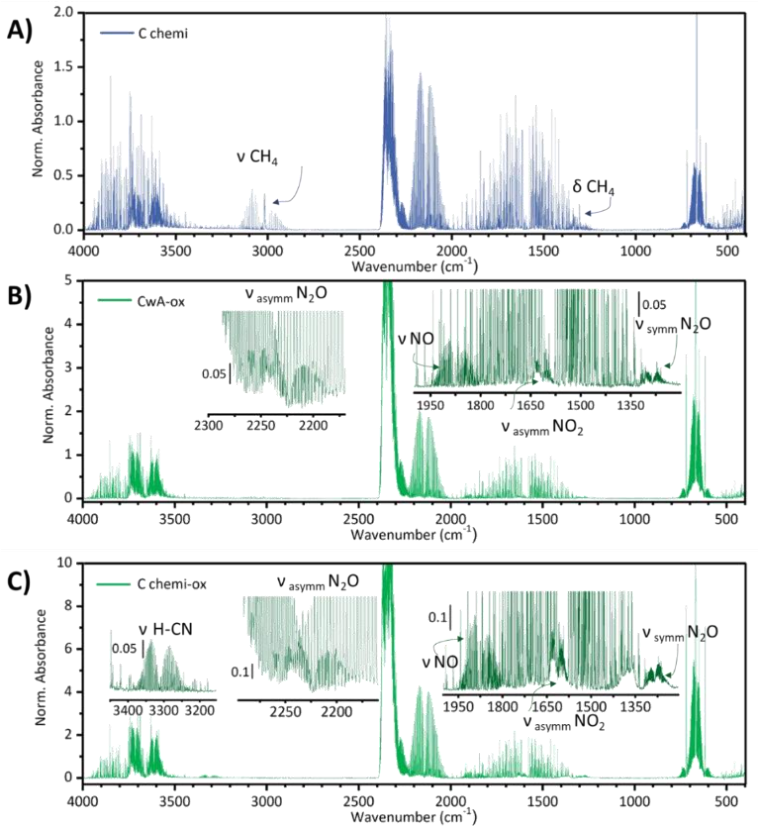

Figure 4: FT-IR spectra collected at the end of the TPD runs on Cchemi (part A), CwA-ox (part B) and Cchemi-ox (part C), normalized to the sample mass. The fingerprints of gases either than CO, CO_2 and H_2O are highlighted.

Table 3: Summary of the mass decrease observed during the TPD runs, reported as a wt % on the initial mass. It reports the total mass lost, the fractions explicable with the detected amounts of CO, CO_2, H_2O, CH_4, NO and SO_2 deriving from the decomposition of functional groups. The NO and SO_2 columns have been duplicated and expressed in terms of N and S (w/w%), so to obtain values directly comparable to those obtained by elemental analysis and reported in Table 1. The last column, calculated by difference, corresponds to the mass lost (w/w%) derived from physisorbed water removed during the activation step at 120 °C overnight.

	Total	**CO**	**CO_2**	**H_2O**	**CH_4**	**NO**	**N**	**SO_2**	**S**	**H_2O-phys**
CwA	6.0	1.0	1.2	0.3	-	-	-	-	-	3.5
CwB	9.3	0.8	1.3	0.4	-	-	-	0.036	0.018	6.8
CpA	12.6	0.6	1.2	0.3	-	-	-	0.063	0.032	10.5
CpB	8.9	0.7	1.2	0.3	-	-	-	0.014	0.007	6.8
Cchemi	13.6	2.7	2.5	1.7	0.1	-	-	-	-	6.6
CwA-ox	23.2	3.8	7.9	1.4	-	0.3	0.15	-	-	9.8
Cchemi-ox	41.7	8.2	16.8	2.5	-	1.0	0.47	-	-	13.2

The FT-IR spectra collected at the end of the TPD runs were used for a quantitative determination of the absolute mass loss (in wt% percentage on the initial mass), and for distributing this mass loss among the quantified products. The quantified mass loss values are fully comparable to the ones measured by TGA, as commented in section S6 in the supporting information. These data are reported for all the investigated carbons in Table 3. The following comments can be done:

1. For all the physically activated carbons the mass loss is less than 10 wt%, except for CpA (12.6 wt%), and the main source of mass loss is the removal of physisorbed water.

2. The mass loss for Cchemi is ca. 1.5 times higher than that observed in average for the physically activated carbons, but only half is due to physisorbed water, while the absolute amount of CO, CO_2 and H_2O released at the end of the experiment is almost 3 times higher. This is also observable by comparing the intensity of the FT-IR spectrum collected at the end of the run on Cchemi (Figure 4A) with those collected for the physically activated carbons (Figure 3).
3. The mass loss is even larger for the two oxidized samples, reaching the value of 41.7 wt% for Cchemi-ox. At the same time, the contribution of physisorbed water to the mass loss gradually decreases (ca. 40-30%), while that of CO, CO_2 and H_2O increases, in agreement with the much larger amount of functional groups expected in the oxidized carbons.
4. Nitrogen is detected by TPD-IR only in the two oxidized carbons, and in much lower amount with respect to elemental analysis. This indicates that the nitrogen functionalities present in the pristine carbons are not thermolabile surface groups, but rather nitrogen is integrated within the graphitic structure of carbon. Oxidation by HNO_3 instead introduces a fraction of N-containing surface groups that decompose at a rather low temperature.
5. TPD-IR has a greater sensibility to lower amounts of sulphur than CHNS elemental analysis. Indeed, sulphur was detected by elemental analysis only on CpA, while TPD-IR quantifies traces of sulphur also in CwB and CpB. However, the total amount of sulphur detected by TPD-IR is lower than that measured by elemental analysis, indicating that only a fraction of the S-functionalities is thermolabile.
6. The amount of physisorbed water determined by TPD-IR is perfectly comparable to that obtained by TGA measurements (Table 1).

3.4 TPD-IR: Gases production rates as a function of temperature

3.4.1 Physically activated carbons

The difference TPD plots (reporting the number of moles of gas evolved between the collection of two consecutive FT-IR spectra) for the four physically activated carbons are shown in Figure 5.

In the low temperature range (T < 400 °C), the main decomposition product is CO_2, which gives a peak around 250 °C. The CO_2 produced below 400 °C is generally attributed to the decomposition of carboxylic acid groups,[36-37, 45-46, 48] and the relative narrowness of this peak suggests that the involved functional groups are energetically very similar. At a closer look, we can notice that all the samples also present a CO and a H_2O peak in correspondence with the CO_2 one, although in lower amounts. The formation of CO at low temperature and in concomitance with the signals of CO_2 was already observed in the past,[8, 45, 63] while the evolution of H_2O in this temperature range was often attributed to the desorption of strongly adsorbed water (for example, hydrogen bonded with the O-containing functional groups) or to the condensation of adjacent functional groups.[8, 47-48] Nevertheless, our observation of a contemporary evolution of CO_2, CO and also H_2O is actually very similar to what observed by Li et al[49] and by Vivo-Vilches et al.[50] In the former article an equal amount of CO and H_2O was observed in this temperature interval and assigned to an alternative decomposition route for carboxylic acids. The latter study instead explained the observation considering the condensation of two vicinal carboxylic groups and their immediate decomposition to CO_2 + CO + H_2O. Our results do not fully support either of these reaction stoichiometries, and

might be interpreted as a combination of multiple processes occurring simultaneously. After reaching a minimum around 400 °C, the release of both CO and CO_2 increases steadily above 400 °C for all the carbons. However, for the Cw samples the amount of released CO is clearly higher than CO_2, particularly for CwA where the evolution rate for CO is approximatively the double than CO_2 at 700 °C. While for the Cp samples, albeit CO is still the main product, its amount is comparable to that of CO_2. In this temperature range the decomposition of anhydrides, lactones and, later on, also phenols and ethers is expected,[36-37, 45-46, 48] and the described differences in the TPD plots for the four samples clearly point to a different distribution of these functional groups, as described in more details in section 3.5. The signal of H_2O, instead, remains stable and low all over the high temperature range for all the four samples. We attribute it to the condensation of vicinal functional groups, likely phenols, and the generally low values suggest a low probability of adjacent functional groups.

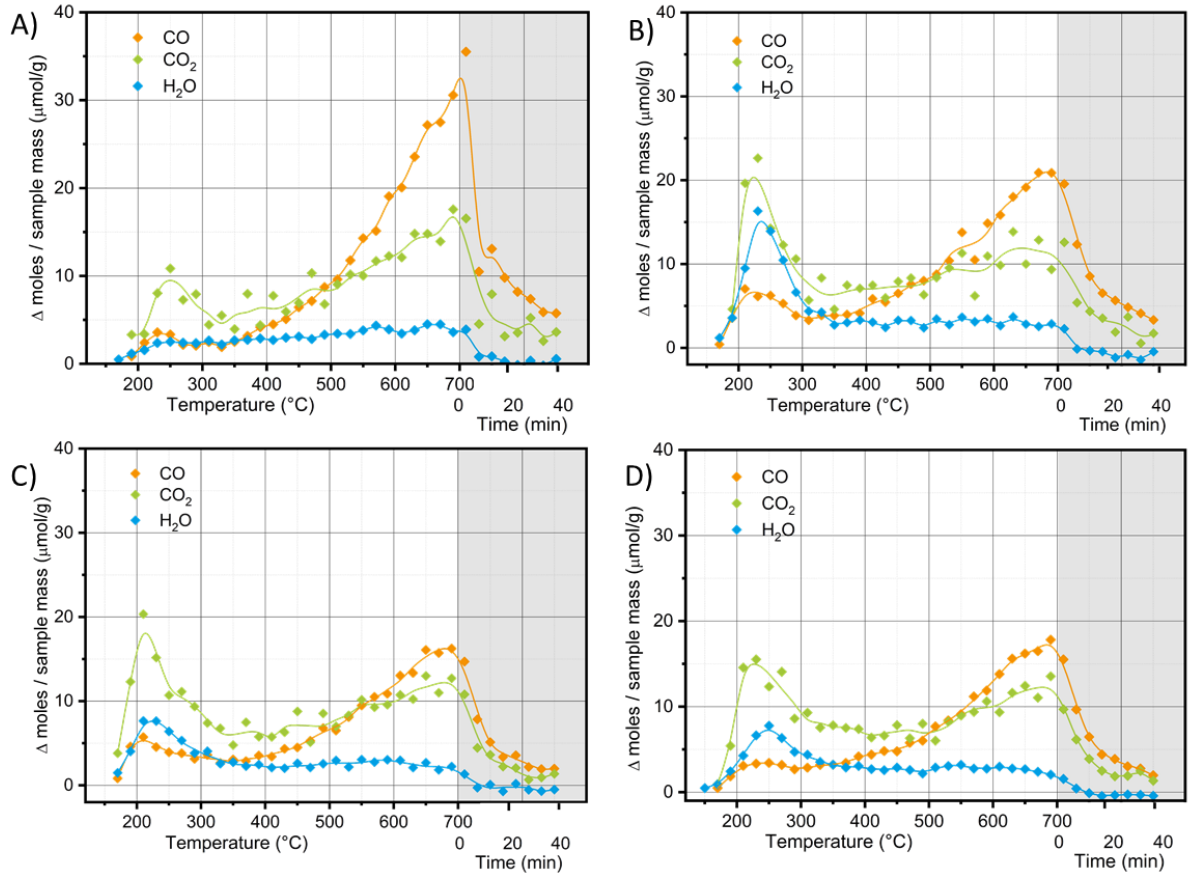

Figure 5: Differential TPD plots of CO, CO_2 and H_2O for the four physically activated carbons: CwA (a), CwB (b), CpA (c) and CpB (d). Each point reports the number of moles of gas evolved by the carbon between the collection of two consecutive IR spectra (i.e. in a temperature interval of 20 °C for the ramp and every 5 min for the isotherm). The data collected during the temperature ramp segment are reported on a white background, while those collected during the isothermal segment are shown on a grey background.

The experimental points associated with the isotherm at 700 °C (grey background in Figure 5) provide further details about the kinetics of the decomposition reactions. As expected, the formation rate of all the products progressively decreases. More interestingly, the formation rate for CO and CO_2 does not drop suddenly to zero, but instead it needs more than 20 min before reaching stable values, suggesting that the thermal decomposition of the functional groups is

kinetically slow and requires additional time before reaching the thermodynamic equilibrium. In contrast, the signal of H_2O drops to zero almost immediately after the beginning of the isotherm segment, suggesting that the condensation of two adjacent phenolic groups is a kinetically faster process.

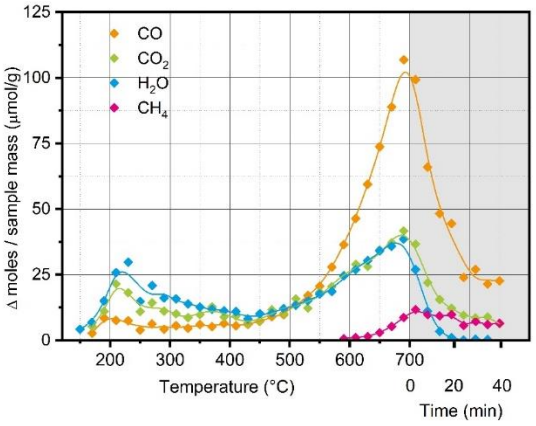

Figure 6: Differential TPD plots of CO, CO_2, H_2O and CH_4 for Cchemi. Each point reports the number of moles of gas evolved by the carbon between the collection of two consecutive IR spectra (i.e. in a temperature interval of 20 °C for the ramp and every 5 min for the isotherm). The data collected during the temperature ramp segment are reported on a white background, while those collected during the isothermal segment are shown on a grey background.

3.4.2 Chemically activated carbon

The differential TPD curves for Cchemi are reported in Figure 6. The general trend is similar to those observed for the physically activated carbons (in particular for CwA), except for the higher intensity. Also in this case the largest release of decomposition products is observed at high temperature, but their amount is sensibly higher than in the previous cases indicating a greater concentration of functional groups. This, in turn, could also explain the relatively greater amount of H_2O released, as it corresponds to greater chances of vicinal functional groups, and consequently to more likely condensation processes.

As anticipated above, CH_4 was observed and quantified among the decomposition products of Cchemi. Its signal appears at about 600 °C and continues to consistently increase all over the final part of the experiment. Cchemi was activated at lower temperature than physically activated carbons, and thus the formation of CH_4 in the TPD indicates that we have surpassed the primitive activation temperature and triggered a further carbonization of the sample.[41] This last process also appears to be kinetically slow, as the production rate of CH_4 does not slow down sensibly during the isothermal segment of the experiment.

3.4.3 Oxidized activated carbons

The differential TPD curves for CwA-ox and Cchemi-ox are reported in Figure 7. A much larger amount of gases is released during the TPD runs with respect to the previous cases. This is expected, since it is known that oxidation by HNO_3 introduces a large amount of O-containing functional groups in carbons.[8-9, 37, 48]

As commonly observed for carbons treated by wet oxidation routes,[8-9, 37] very large amounts of CO_2, CO and H_2O are released in the low temperature interval. As discussed above, the formation of CO_2 below 400 °C is attributed to the decomposition of carboxylic acid groups. It is worth noticing

that the CO_2 peak is much broader than in the previous cases, suggesting a wider distribution of carboxylic acid groups in comparison with the non-oxidized carbons. Also for CwA-ox and Cchemi-ox, CO and H_2O are released simultaneously to CO_2. Here, the moles of CO and H_2O produced over this interval are very similar, supporting the alternative decomposition mechanism of carboxylic acid groups proposed by Li et al,[49] or the decomposition of two vicinal COOH groups proposed by Vivo-Vilches et al.[50]

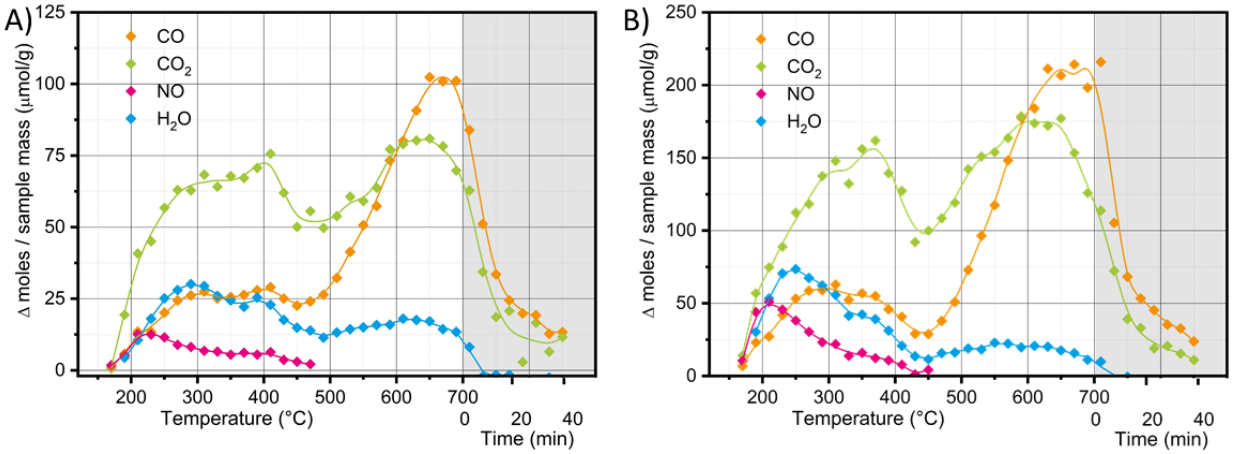

Figure 7: Differential TPD plots of CO, CO_2, H_2O and NO for CwA-Ox (a) and Cchemi-Ox (b). Each point reports the number of moles of gas evolved by the carbon between the collection of two consecutive IR spectra (i.e. in a temperature interval of 20 °C for the ramp and every 5 min for the isotherm). The data collected during the temperature ramp segment are reported on a white background, while those collected during the isothermal segment are shown on a grey background.

In addition to CO, CO_2 and H_2O, nitrogen oxides are released at low temperature. In particular, NO was identified and quantified for both samples, but the IR spectra identified also NO_2 (1615 cm^{-1}), N_2O (2223 and 1285 cm^{-1}) and HCN (3310 cm^{-1}). The presence of these gases clearly indicates the introduction of N-containing functional groups as a consequence of the oxidation treatment in HNO_3.

For both carbons, the release rates of all products reach a minimum at about 450 °C, and then quickly rise again as the decomposition of the more thermostable functional groups starts. With respect to the parent carbons (CwA and Cchemi), a significant increase of the amounts of released CO and CO_2 is observed. In contrast, CH_4 is not observed at all in any of the oxidized samples. CH_4 is expected to be formed by carbonization processes of residual aliphatic fractions within the carbon sample. Its absence confirms the fact that the aliphatic fraction is the most vulnerable to the action of oxidative agents, such as HNO_3.[64]

3.5 TPD-IR: quantitative evaluation of the functional groups concentration

The data reported in the differential TPD plots discussed above were used to quantify the amount of gases (in µmol/g) released by a given carbon during three temperature intervals characteristic for the decomposition of different classes of functional groups, as reported in Table 3. These data were used to obtain a reasonable estimation of the concentration of different functional groups in the activated carbons, on the basis of the available literature[36-37, 45-46, 48-50] and of the following assumptions.

1. Carboxylic acids decompose at temperatures lower than 400 °C, mainly releasing CO_2, but also alternative decomposition routes involving the contemporary formation of CO and H_2O[49] or CO, CO_2 and H_2O[50] were proposed and appeared compatible with the TPD plots discussed in section 3.4. Keeping this is mind, we evaluated the concentration of carboxylic acids by summing the µmol/g of CO_2 and CO released in the T < 400 °C interval. An amount of H_2O equal to the released CO is expected to be associated with the decomposition of carboxylic groups as well, while the remaining part is attributed to condensation reactions among vicinal groups or to strongly adsorbed H_2O. Finally, NO is fully attributed to the decomposition of N-containing functional groups such as, for example, nitro groups.
2. Anhydrides and lactones are the only species expected to decompose in the 400 – 560 °C interval. The former decomposes to CO_2 + CO, while the latter to CO_2 only. Thus, the µmol/g of CO released in this interval can only be attributed to the decomposition of anhydrides, while the concentration of the most thermolabile faction of lactones is estimated by subtracting the concentration of anhydrides to the total amount of CO_2 evolved in this interval. All the water observed in this range is attributed to the condensation of vicinal functional groups, most likely phenols.
3. In the high temperature range (560 – 700 °C) the decomposition of lactones continues for the most of the interval, but in addition also the decomposition of phenols and ethers to CO becomes possible. Lactones decomposing in this interval can be univocally quantified by the µmol/g of CO_2 released, so that the total amount of lactones in each sample can be determined by summing the values obtained in the medium and high temperature intervals. The amount of CO released gives an estimation of the total amount of phenols and ethers, which cannot be discriminated.

Table 4: Summary of the amounts (in µmol/g) of CO, CO_2, H_2O, NO and CH_4 released by each carbon during the TPD run. The values are divided into the T < 400 °C, 400 °C < T < 560 °C and T > 560 °C intervals.

	T < 400 °C				**400 °C < T < 560 °C**				**T > 560 °C**			
	CO	**CO_2**	**H_2O**	**NO**	**CO**	**CO_2**	**H_2O**	**NO**	**CO**	**CO_2**	**H_2O**	**CH_4**
CwA	29	68	28	-	68	67	26	-	259	144	35	-
CwB	52	116	80	-	66	65	24	-	185	107	19	-
CpA	43	117	53	-	48	60	20	-	136	103	16	-
CpB	35	111	53	-	51	58	22	-	151	108	18	-
Cchemi	70	152	207	-	89	92	98	-	793	335	249	89
CwA-ox	238	630	246	92	252	467	123	15	864	703	100	-
Cchemi-ox	546	1345	581	321	474	994	138	13	1920	1469	110	-

The concentration values obtained by this evaluation are reported in Figure 8. For the physically activated carbons (inset in Figure 8), albeit the low concentration of functional groups, we are able to point out analogies and differences among the four samples. The two carbons of wood origin (CwA and CwB) display a different distribution of the functional groups: phenols + ethers are the most abundant functional groups in CwA, followed by lactones, carboxylic acids and, at last, anhydrides. In CwB, instead, an almost equal amount of carboxylic acids and phenols + ethers are observed. The two carbons of peat origin (CpA and CpB) are more similar each others. The concentration of carboxylic acids, anhydrides and lactones is similar to CwB, while they contain less

phenols and ethers. Finally, the amount of water attributed to condensation reactions among vicinal functional groups is very low in all the four carbons, in particular for the Cp samples, and thus the amount of anhydrides, lactones or ethers formed as a consequence of a condensation reaction during the TPD run is expected to be low.

For Cchemi the concentration of functional groups is roughly three times that estimated for the physically activated samples. Also the relative distribution of the functional groups in Cchemi is different with respect to the physically activated carbons: phenols and ethers are the most abundant, followed by lactones, carboxylic acids and anhydrides. Cchemi also provided a very high amount of released water, suggesting that the condensation of vicinal functional groups is the most likely for this sample.

For the samples oxidised in HNO_3 (CwA-ox and Cchemi-ox), the overall concentration of functional groups increases with respect to the parent carbons. Cchemi-ox has roughly the double of functional groups than CwA-ox, but their relative amounts are similar. In both cases, very similar amounts of lactones, carboxylic acids and, phenols + ethers are observed, while the concentration of anhydrides is significantly lower. The amount of released water is small in comparison with that of any of the observed functional groups, suggesting that the fraction of functional groups formed by the condensation of vicinal groups during the TPD run can be considered almost negligible for these samples.

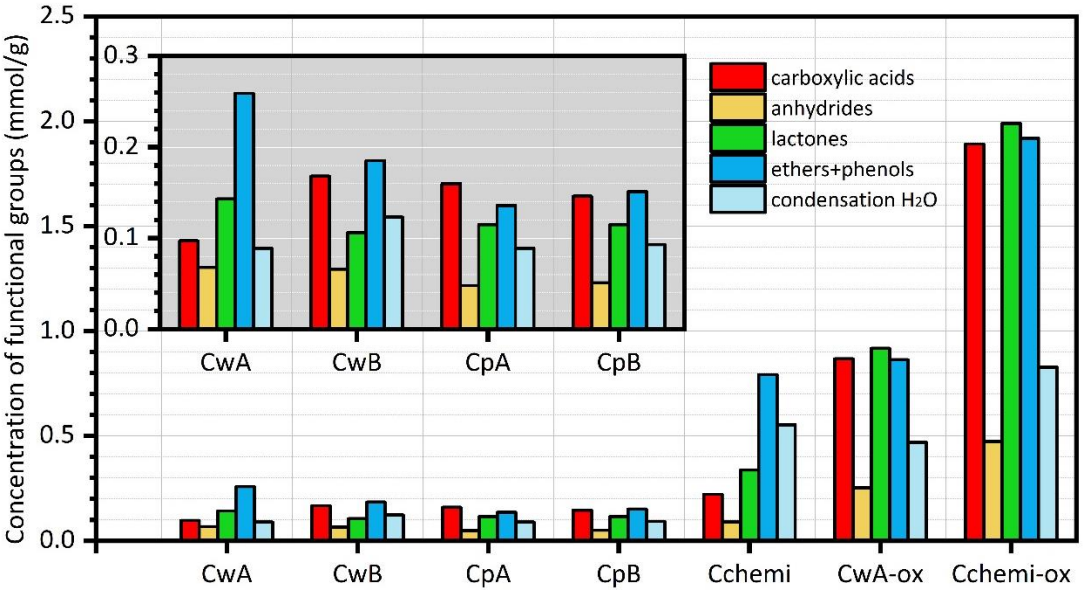

Figure 8: Concentration of functional groups in the seven activated carbons, as evaluated from the measured amounts of released gases in the TPD-IR experiments. A detail over the values calculated for the physically activated carbons is shown in the inset.

3.6 Attempts to combine TPD-IR, Boehm titration, TGA, elemental analysis and XPS: a critical discussion

For carboxylic acids, anhydrides and lactones, the values determined by TPD-IR can be compared with those estimated by Boehm titration (Section 3.2 and Table 2). Figure 9 shows the two series of data plotted in the same graphs for carboxylic acids + anhydrides (part A) and lactones (part B): data lying on the bisector indicate that the two methods give the same results. The carbons investigated

in this work can be divided in two main groups (shown as blue and orange points, respectively). For parent carbons, i.e. having a low or moderate amount of surface functional groups decomposing below 700 °C (below 1.5 mmol/g), the two methods quantify a similar (although not the same) amount of functional groups. In contrast, for HNO_3-oxidised carbons Boehm titration systematically underestimates the amount of functional groups with respect to TPD-IR. This is due to the intrinsic (and already reported) limitation of the Boehm titration method, as discussed in Section 3.2: the presence of water as a solvent limits the accessibility of the functional groups to the base, the more the higher is the amount of functional groups. On a more quantitative ground, a linear fit of the data related to pristine carbons (dotted lines in Figure 9) gives a good result for carboxylic acids + anhydrides (R^2 = 0.88), while the fit is rather scarce for lactones (R^2 = 0.63). However, we notice that by removing CwA from the two series of data, both fits greatly improve (R^2 = 0.98 and 0.96, respectively, Figure S6). The reason why CwA goes out of the trend is under investigation. Nevertheless, Figure 9 suggests that our TPD-IR approach, on average, may give results comparable with those obtained by Boehm titration for carbon materials having a low or moderate amount of surface functional groups.

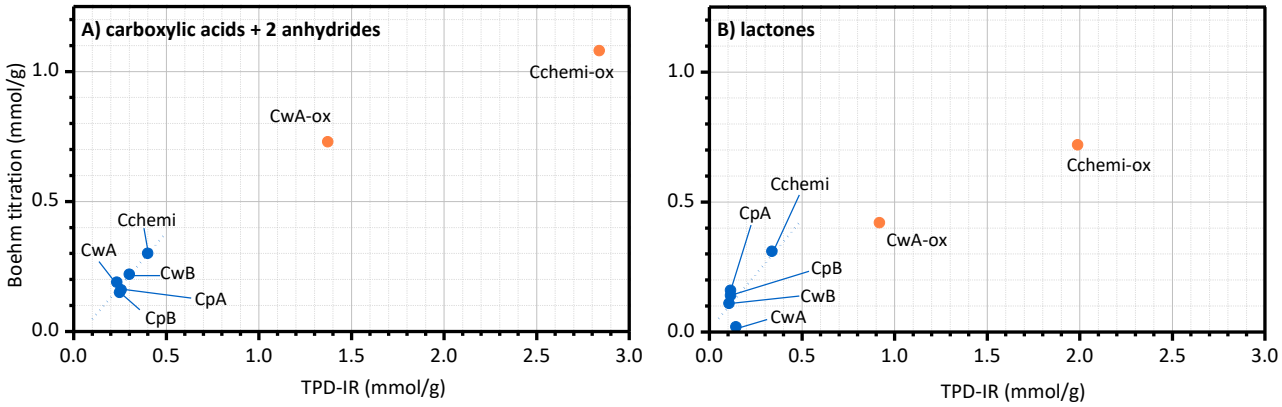

Figure 9: Concentration of carboxylic acids + 2 anhydrides (part A) and lactones (part B) as determined by TPD-IR plotted against the same values obtained by Boehm titration. Two different trends can be observed, one for the physically activated carbons and Cchemi (blue), and one for the two oxidized carbons (orange). The linear fit for the pristine carbons is reported as dotted blue line (R^2 = 0.88 and 0.63 for parts A and B, respectively). The same fits performed after excluding CwA from the series greatly improved, as reported in Figure S6.

Since the main drawback of our TPD-IR setup relies in the impossibility to quantify in a direct way the functional groups decomposing at T > 700 °C, we attempted to obtain a rough estimation of the amount of these groups by comparing all the data at our disposal. Indeed, elemental analysis provides an estimation of the total oxygen content (including that belonging to physisorbed water), TGA gives the amount of physisorbed water, and from TPD-IR we can calculate the amount of oxygen belonging to those functional groups that decompose below 700 °C. The difference between these three oxygen concentrations corresponds to the amount of oxygen belonging to species which are stable up to 700 °C, among which ketones and quinones (i.e. carbonyls) are probably the most abundant. We found that for all the physically activated carbons, the amount carbonyls is by far higher than the amount of all the other oxygen functional, although the relative ratio changes from carbon to carbon. In particular, in carbons of wood origin oxygen belonging to carbonyls is 2 times higher than oxygen belonging to all the other functional groups, while in carbons of peat origin it is

4-5 times greater, accounting for a greater total amount of oxygen. Even though the absolute numbers might be affected by the many approximations, this is in agreement with the average higher hydrophilicity of peat carbons with respect to wood carbons, as reported in Table 3. When comparing CwA and Cchemi, the total amount of oxygen is almost double in Cchemi, which is in agreement with previously reported XPS data, according to which the relative atomic concentration O/C in Cchemi was about double than that of CwA.[26] On the other hand, according to our comparative analysis, in the oxidized carbons the relative amount of functional groups decomposing below 700 °C drastically increases with respect to carbonyls. Without wanting to overanalyze this result, it indicates that the functional groups generated by HNO_3-oxidation are mainly thermolabile groups. This is again in qualitative agreement with previous XPS data, which indicated that the acid treatment caused an increase of the peak assigned to carboxyl, lactone and ester groups, at the expenses of the peak ascribed to graphitic sp^2 carbon.[18]

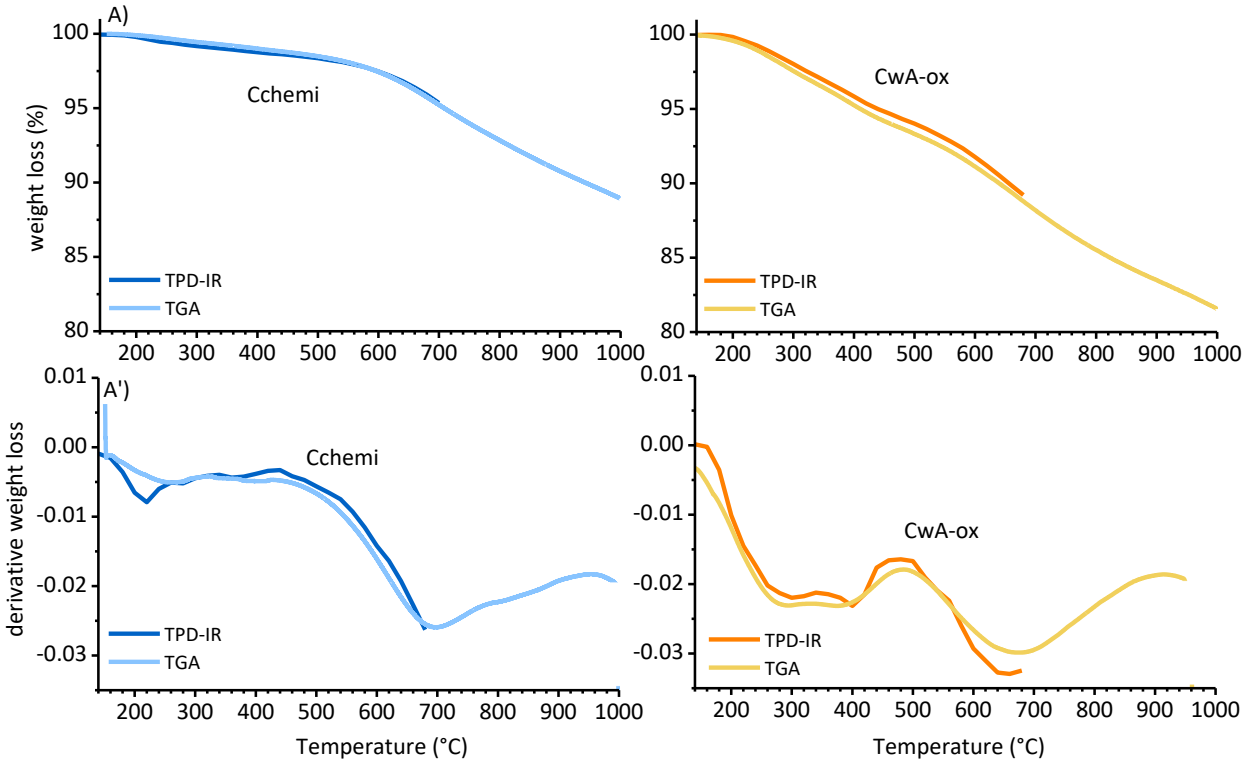

Figure 10: Comparison between the weight-loss as a function of the temperature in Cchemi (part A and A') and CwA-ox (B and B'), as evaluated with the TPD-IR setup described in this work and with standard TGA. Both the weight loss % (part A and B) and their first derivatives (A' and B') are shown.

For Cchemi and CwA-ox (chosen as representative of carbons having a low and high amount of surface functional groups decomposing below 700 °C, respectively) the amount of thermal decomposition products at a temperature higher than 700 °C (i.e. carbonyls) was also evaluated in terms of weight loss by TGA, as reported in Figure 10. For both samples, striking similarities were observed between the weight loss measured by TPD-IR and TGA, both in terms of absolute weight loss values and of the trends of the first derivative. This confirms that our TPD-IR analysis quantifies correctly the amount of gaseous decomposition products evolved during the experiment and that the thermal decomposition processes occurring in the TPD-IR apparatus (static vacuum conditions

with gases accumulation) is analogous to the one happening in the TGA one (inert gas flux conditions). Furthermore, the TGA measurements are not constrained to the 700 °C threshold as our TPD-IR setup, allowing to evaluate the mass of the decomposition products produced in the 700 – 1000 °C range. In this respect we can observe that Cchemi has a lower weight loss in the 120 – 700 °C temperature range than in the 700 – 1000 °C one (4.8 and 6.3%, respectively). For the oxidised CwA-ox sample instead the ratio is reversed, with a weight loss of 11.8 % in the 120 -700 °C temperature range and of 6.6% at higher temperature. This trend is again consistent with the rough evaluation of the mmol/g of oxygen decomposed by these two samples at temperatures lower and higher than 700 °C, as obtained by combining TPD-IR, EA and TGA data: also in that case, for Cchemi the amount of products lost above 700 °C (i.e. carbonyls) was remarkably higher than at lower temperature, while the reverse was observed for CwA-ox.

Finally, in this comparative section it is interesting to notice that the analysis discussed above does not completely agree with the speciation of oxygen-containing functional groups as determined by our previous XPS analysis.[18,26] In particular, the relative amount of carbonyls determined by XPS (the only functional group which can be univocally speciated) is greatly underestimated for all the analysed carbons, and especially for the pristine ones. Without wishing to judge one technique better than the other, we limit to observe that TGA measurements up to 1000 °C (Figure 10) have shown that Cchemi loses more weight (6.2 wt%) above 700 °C than below (4.3 wt%), which means that it contains more carbonyls than all the other functional groups. These numbers are in fair agreement with our analysis of the TPD-IR data, according to which the carbonyls account for 6.3 wt% loss, and all the other groups for 4.8 wt%. In contrast, XPS estimates that carbonyls are much less than all the other functional groups (accounting for only 15% of the total). A similar situation is found for CwA-ox. TGA measurements up to 1000 °C (Figure 10) indicated that the weight loss above 700 °C is approximately half of that below 700 °C, which is again in fair agreement with the analysis of the TPD-IR results, according to which the fraction of functional groups decomposing above 700 °C is 0.4 times that of the groups decomposing below 700 °C. Again, these values do not match with the speciation determined by previous XPS analysis, which indicated that carbonyls are 6 times less than all the other groups. Although we cannot exclude some bias in our TPD-IR analysis, at least part of the disagreement might be explained by the already discussed intrinsic difficulties of XPS in quantifying oxygen groups in microporous carbons,[16, 23-24] among which the most relevant ones are the difficulty to probe groups at the internal surface and the fact that some groups (e.g. lactones) are counted twice (since they contribute simultaneously at two different peaks in the spectrum).

4. Conclusions

Activated carbons play a key role in many catalytic applications. The possibility of tuning their surface chemistry by changing the carbonaceous precursor and/or the activation treatment is the origin of much industrial and fundamental research carried out over the last decade. However, due to their intrinsic structural heterogeneity, the characterization of the nature and amount of surface groups in activated carbons is not straightforward. In this work, we presented the potentials of a multi-technique approach, relying on an alternative TPD-IR approach, TGA, elemental analysis and Boehm titration measurements, to identify and quantify the functional groups in activated carbons. Our own TPD-IR experimental set-up has several advantages: it is very simple, versatile and achievable by standard lab equipment, it operates in accumulation, but still at very low partial pressures and hence minimizes the occurrence of secondary reactions, it allows for the measurement of high-resolution IR spectra, it is fully suitable for the identification of the IR-active gases released at high concentration as well as of those produced at traces levels and for the quantification of the main products.

The quantified amounts of gaseous products were used for estimating the concentration of the main functional groups in seven carbons characterized by different precursors (wood or peat), activation procedure (physical activation by steam or chemical activation with H_3PO_4) and post-activation treatments (oxidation in HNO_3). The so obtained values were analysed in conjunction with results from elemental analysis, TGA and Boehm titration measurements, which allowed us to critically discuss advantages/disadvantages of each technique. The main results can be summarized as follows.

1. Even though for the four steam activated carbons (CwA, CwB, CpA and CpB) the estimated concentration of functional groups is low (below 10 mmol/g), significant differences in their relative amount are observed. In carbons of wood origin, O-containing functional groups decomposing below 700 °C are about one half of those decomposing above (ketones and quinones) and are mostly ethers and phenols, followed by lactones, carboxylic acids and, at a minor extent, anhydrides. In carbons of peat origin, instead, ketones and quinones are 4-5 times more abundant than functional groups decomposing below 700 °C, which are almost equally distributed among carboxylic acids, lactones, ethers and phenols. As far as other functional groups are concerned, nitrogen is detected by elemental analysis in all the four physically activated carbons. The absence of N-containing gases in TPD-IR indicates that this nitrogen is covalently bonded within the graphitic structure. Traces of thermolabile S-groups have been found in all the steam-activated carbons except CwA by TPD-IR, which demonstrated a much higher sensitivity than elemental analysis. On the other hand, the higher concentration of S measured by EA than the one obtained by TPD-IR suggests the presence of a strongly bonded and thermoresistant S fraction in the sample.
2. The chemically activated carbon exhibits a total amount of O-containing functional groups comparable to carbons of peat origin, but in this case they are almost equally distributed among those decomposing below and above 700 °C (i.e. the groups decomposing below 700 °C are about three times more than in steam-activated carbons). As far as their distribution is concerned, ethers and phenols are the most abundant, followed by lactones and carboxylic acids. Condensation of vicinal functional groups with release of H_2O occurs at a large extent.

A quantifiable amount of CH_4 is also released above 600 °C. The observation of this signal, together with its absence in the corresponding oxidized sample, suggest that the chemically activated carbon contains a larger fraction of aliphatic groups than the steam activated carbons.

3. Finally, the two carbons oxidized in HNO_3 contain a larger amount of O-containing functional groups decomposing below 700 °C. Lactones, carboxylic acids and ethers + phenols are present in almost equal amount. Oxidation by HNO_3 introduces also N-containing functional groups, partially in the form of oxidized nitrogen at the edges, that decompose at rather low temperature, and others incorporated into the graphitic structure, which are stable at least until 700 °C.

Overall, our alternative TPD-IR approach appears as a promising and versatile new option to identify and quantify the surface functional groups on different carbon materials. It allows for the precise quantification of the CO and CO_2 products, as well as for a good estimation of the released H_2O as a function of temperature, at the same time allowing for the detection of minor species with possible relevance in catalysis. Coupling these information with those obtained by complementary analytical methods, and in particular elemental analysis, TGA, Boehm titration and XPS, it might be possible to describe the distribution of surface functional groups in carbon materials. We provided some independent evidence which seem to corroborate this approach, while we noticed some inconsistencies with previous XPS analysis on some of the same samples, which however can be accounted for the known intrinsic difficulties of XPS in correctly quantifying surface functional groups in microporous carbons. We are aware that this type of characterisation remains a challenging task and that our approach may still require a wider and more thorough validation. We hope that in the near future it might be tested and eventually validated by other research groups involved in the study of the surface chemistry of carbon materials. At the same time, the present work offers many points of reflection on the pros and cons of the techniques conventionally used for the characterization of carbonaceous materials.

Acknowledgements

We are particularly grateful to Andrea Governini (Chimet SpA) for the Boehm titrations, and to Fabrizio Caldera (Department of Chemistry at the University of Torino) for the help in elemental analysis measurements.

Conflicts of interest

There are no conflicts to declare.

References

1. Fierro, V.; Torné-Fernández, V.; Montané, D.; Celzard, A., Adsorption of phenol onto activated carbons having different textural and surface properties. *Microporous and Mesoporous Materials* **2008,** *111* (1), 276-284.
2. Sircar, S.; Golden, T. C.; Rao, M. B., Activated carbon for gas separation and storage. *Carbon* **1996,** *34* (1), 1-12.
3. Auer, E.; Freund, A.; Pietsch, J.; Tacke, T., Carbons as supports for industrial precious metal catalysts. *Applied Catalysis A: General* **1998,** *173* (2), 259-271.
4. Rodríguez-Reinoso, F., Production and Applications of Activated Carbons. *Handbook of Porous Solids* **2002**, 1766-1827.
5. González-García, P., Activated carbon from lignocellulosics precursors: A review of the synthesis methods, characterization techniques and applications. *Renewable and Sustainable Energy Reviews* **2018,** *82*, 1393-1414.
6. Radovic, L. R.; Rodríguez-Reinoso, F., Carbon Materials in Catalysis. In *Chemistry and Physics of Carbon*, 1st ed.; Thrower, P. A.; Dekker, M., Eds. Taylor & Francis: New York, 1997; Vol. 25, pp 243–358.
7. Serp, P.; Figueiredo, J. L., *Carbon Materials for Catalysis*. Wiley & Sons: Hoboken, NJ, 2009.
8. Moreno-Castilla, C.; Carrasco-Marín, F.; Mueden, A., The creation of acid carbon surfaces by treatment with (NH4)2S2O8. *Carbon* **1997,** *35* (10), 1619-1626.
9. Silva, A. M. T.; Machado, B. F.; Figueiredo, J. L.; Faria, J. L., Controlling the surface chemistry of carbon xerogels using HNO3-hydrothermal oxidation. *Carbon* **2009,** *47* (7), 1670-1679.
10. Bhatnagar, A.; Hogland, W.; Marques, M.; Sillanpää, M., An overview of the modification methods of activated carbon for its water treatment applications. *Chemical Engineering Journal* **2013,** *219*, 499-511.
11. Rodrigues, R.; Gonçalves, M.; Mandelli, D.; Pescarmona, P. P.; Carvalho, W. A., Solvent-free conversion of glycerol to solketal catalysed by activated carbons functionalised with acid groups. *Catalysis Science & Technology* **2014,** *4* (8), 2293-2301.
12. Girgis, B. S.; Yunis, S. S.; Soliman, A. M., Characteristics of activated carbon from peanut hulls in relation to conditions of preparation. *Materials Letters* **2002,** *57* (1), 164-172.
13. Miguel, G. S.; Fowler, G. D.; Dall'Orso, M.; Sollars, C. J., Porosity and surface characteristics of activated carbons produced from waste tyre rubber. *Journal of Chemical Technology & Biotechnology* **2002,** *77* (1), 1-8.
14. Biniak, S.; Szymański, G.; Siedlewski, J.; Światkoski, A., The characterization of activated carbons with oxygen and nitrogen surface groups. *Carbon* **1997,** *35* (12), 1799-1810.
15. Jaramillo, J.; Álvarez, P. M.; Gómez-Serrano, V., Oxidation of activated carbon by dry and wet methods: Surface chemistry and textural modifications. *Fuel Processing Technology* **2010,** *91* (11), 1768-1775.
16. Figueiredo, J. L., Functionalization of porous carbons for catalytic applications. *Journal of Materials Chemistry A* **2013,** *1* (33), 9351-9364.
17. Figueiredo, J. L.; Pereira, M. F. R., The role of surface chemistry in catalysis with carbons. *Catalysis Today* **2010,** *150* (1), 2-7.
18. Lazzarini, A.; Pellegrini, R.; Piovano, A.; Rudić, S.; Castan-Guerrero, C.; Torelli, P.; Chierotti, M. R.; Gobetto, R.; Lamberti, C.; Groppo, E., The effect of surface chemistry on the performances of Pd-based catalysts supported on activated carbons. *Catalysis Science & Technology* **2017,** *7* (18), 4162-4172.
19. Pérez-Mayoral, E.; Calvino-Casilda, V.; Soriano, E., Metal-supported carbon-based materials: opportunities and challenges in the synthesis of valuable products. *Catalysis Science & Technology* **2016,** *6* (5), 1265-1291.
20. Boehm, H. P., Some aspects of the surface chemistry of carbon blacks and other carbons. *Carbon* **1994,** *32* (5), 759-769.
21. Boehm, H. P., Chemical Identification of Surface Groups. In *Advances in Catalysis*, Eley, D. D.; Pines, H.; Weisz, P. B., Eds. Academic Press: 1966; Vol. 16, pp 179-274.

22. Smith, M.; Scudiero, L.; Espinal, J.; McEwen, J.-S.; Garcia-Perez, M., Improving the deconvolution and interpretation of XPS spectra from chars by ab initio calculations. *Carbon* **2016,** *110*, 155-171.
23. Konno, H., Chapter 8 - X-ray Photoelectron Spectroscopy. In *Materials Science and Engineering of Carbon*, Inagaki, M.; Kang, F., Eds. Butterworth-Heinemann: 2016; pp 153-171.
24. Lennon, D.; Lundie, D. T.; Jackson, S. D.; Kelly, G. J.; Parker, S. F., Characterization of Activated Carbon Using X-ray Photoelectron Spectroscopy and Inelastic Neutron Scattering Spectroscopy. *Langmuir* **2002,** *18* (12), 4667-4673.
25. Dandekar, A.; Baker, R. T. K.; Vannice, M. A., Characterization of activated carbon, graphitized carbon fibers and synthetic diamond powder using TPD and DRIFTS. *Carbon* **1998,** *36* (12), 1821-1831.
26. Lazzarini, A.; Piovano, A.; Pellegrini, R.; Leofanti, G.; Agostini, G.; Rudić, S.; Chierotti, M. R.; Gobetto, R.; Battiato, A.; Spoto, G.; Zecchina, A.; Lamberti, C.; Groppo, E., A comprehensive approach to investigate the structural and surface properties of activated carbons and related Pd-based catalysts. *Catalysis Science & Technology* **2016,** *6* (13), 4910-4922.
27. Vottero, E.; Carosso, M.; Jiménez-Ruiz, M.; Pellegrini, R.; Groppo, E.; Piovano, A., How do the graphenic domains terminate in activated carbons and carbon-supported metal catalysts? *Carbon* **2020,** *169*, 357-369.
28. Carosso, M.; Lazzarini, A.; Piovano, A.; Pellegrini, R.; Morandi, S.; Manzoli, M.; Vitillo, J. G.; Ruiz, M. J.; Lamberti, C.; Groppo, E., Looking for the active hydrogen species in a 5 wt% Pt/C catalyst: a challenge for inelastic neutron scattering. *Faraday Discussions* **2018,** *208* (0), 227-242.
29. Ferrari, A. C.; Robertson, J., Interpretation of Raman spectra of disordered and amorphous carbon. *Physical Review B* **2000,** *61* (20), 14095-14107.
30. Lónyi, F.; Valyon, J., On the interpretation of the NH3-TPD patterns of H-ZSM-5 and H-mordenite. *Microporous and Mesoporous Materials* **2001,** *47* (2), 293-301.
31. Boujana, S.; Demri, D.; Cressely, J.; Kiennemann, A.; Hindermann, J. P., FT-IR and TPD studies on support-metal and promoter-metal interaction. Pt and Pd catalysts. *Catalysis Letters* **1990,** *7* (5), 359-366.
32. Joly, J. P.; Gaillard, F.; Peillex, E.; Romand, M., Temperature-programmed desorption (TPD) of water from iron, chromium, nickel and 304L stainless steel. *Vacuum* **2000,** *59* (4), 854-867.
33. Phung, T. K.; Garbarino, G., On the use of infrared spectrometer as detector for Temperature Programmed (TP) techniques in catalysts characterization. *Journal of Industrial and Engineering Chemistry* **2017,** *47*, 288-296.
34. Zhuang, Q. L.; Kyotani, T.; Tomita, A., DRIFT and TK/TPD Analyses of Surface Oxygen Complexes Formed during Carbon Gasification. *Energy & Fuels* **1994,** *8* (3), 714-718.
35. Zhuang, Q. L.; Kyotani, T.; Tomita, A., The change of TPD pattern of O2-gasified carbon upon air exposure. *Carbon* **1994,** *32* (3), 539-540.
36. de la Puente, G.; Pis, J. J.; Menéndez, J. A.; Grange, P., Thermal stability of oxygenated functions in activated carbons. *Journal of Analytical and Applied Pyrolysis* **1997,** *43* (2), 125-138.
37. Figueiredo, J. L.; Pereira, M. F. R.; Freitas, M. M. A.; Órfão, J. J. M., Modification of the surface chemistry of activated carbons. *Carbon* **1999,** *37* (9), 1379-1389.
38. Szymański, G. S.; Karpiński, Z.; Biniak, S.; Świątkowski, A., The effect of the gradual thermal decomposition of surface oxygen species on the chemical and catalytic properties of oxidized activated carbon. *Carbon* **2002,** *40* (14), 2627-2639.
39. Zhou, J.-H.; Sui, Z.-J.; Zhu, J.; Li, P.; Chen, D.; Dai, Y.-C.; Yuan, W.-K., Characterization of surface oxygen complexes on carbon nanofibers by TPD, XPS and FT-IR. *Carbon* **2007,** *45* (4), 785-796.
40. Diyuk, V. E.; Mariychuk, R. T.; Lisnyak, V. V., Barothermal preparation and characterization of micro-mesoporous activated carbons. *Journal of Thermal Analysis and Calorimetry* **2016,** *124* (2), 1119-1130.
41. Hotová, G.; Slovák, V.; Soares, O. S. G. P.; Figueiredo, J. L.; Pereira, M. F. R., Oxygen surface groups analysis of carbonaceous samples pyrolysed at low temperature. *Carbon* **2018,** *134*, 255-263.

42. Ishii, T.; Kashihara, S.; Hoshikawa, Y.; Ozaki, J.-i.; Kannari, N.; Takai, K.; Enoki, T.; Kyotani, T., A quantitative analysis of carbon edge sites and an estimation of graphene sheet size in high-temperature treated, non-porous carbons. *Carbon* **2014,** *80*, 135-145.
43. Ishii, T.; Kyotani, T., Chapter 14 - Temperature Programmed Desorption. In *Materials Science and Engineering of Carbon*, Inagaki, M.; Kang, F., Eds. Butterworth-Heinemann: 2016; pp 287-305.
44. Ishii, T.; Ozaki, J. I., Understanding the chemical structure of carbon edge sites by using deuterium-labeled temperature-programmed desorption technique. *Carbon* **2020,** *161*, 343-349.
45. Figueiredo, J. L.; Pereira, M. F. R.; Freitas, M. M. A.; Órfão, J. J. M., Characterization of Active Sites on Carbon Catalysts. *Industrial & Engineering Chemistry Research* **2007,** *46* (12), 4110-4115.
46. Moreno-Castilla, C.; Carrasco-Marín, F.; Maldonado-Hódar, F. J.; Rivera-Utrilla, J., Effects of non-oxidant and oxidant acid treatments on the surface properties of an activated carbon with very low ash content. *Carbon* **1998,** *36* (1), 145-151.
47. Haydar, S.; Moreno-Castilla, C.; Ferro-García, M. A.; Carrasco-Marín, F.; Rivera-Utrilla, J.; Perrard, A.; Joly, J. P., Regularities in the temperature-programmed desorption spectra of CO2 and CO from activated carbons. *Carbon* **2000,** *38* (9), 1297-1308.
48. Otake, Y.; Jenkins, R. G., Characterization of oxygen-containing surface complexes created on a microporous carbon by air and nitric acid treatment. *Carbon* **1993,** *31* (1), 109-121.
49. Li, N.; Ma, X.; Zha, Q.; Kim, K.; Chen, Y.; Song, C., Maximizing the number of oxygen-containing functional groups on activated carbon by using ammonium persulfate and improving the temperature-programmed desorption characterization of carbon surface chemistry. *Carbon* **2011,** *49* (15), 5002-5013.
50. Vivo-Vilches, J. F.; Bailón-García, E.; Pérez-Cadenas, A. F.; Carrasco-Marín, F.; Maldonado-Hódar, F. J., Tailoring the surface chemistry and porosity of activated carbons: Evidence of reorganization and mobility of oxygenated surface groups. *Carbon* **2014,** *68*, 520-530.
51. Zielke, U.; Hüttinger, K. J.; Hoffman, W. P., Surface-oxidized carbon fibers: I. Surface structure and chemistry. *Carbon* **1996,** *34* (8), 983-998.
52. Zhang, L. H.; Calo, J. M., Thermal desorption methods for porosity characterization of carbons and chars. *Colloids and Surfaces A: Physicochemical and Engineering Aspects* **2001,** *187-188*, 207-218.
53. Marchon, B.; Tysoe, W. T.; Carrazza, J.; Heinemann, H.; Somorjai, G. A., Reactive and kinetic properties of carbon monoxide and carbon dioxide on a graphite surface. *The Journal of Physical Chemistry* **1988,** *92* (20), 5744-5749.
54. Haydar, S.; Joly, J. P., Study of the Evolution of Carbon Dioxide from Active Carbon by a Threshold Temperature-Programmed Desorption Method. *Journal of Thermal Analysis and Calorimetry* **1998,** *52* (2), 345-353.
55. Jung, I.; Field, D. A.; Clark, N. J.; Zhu, Y.; Yang, D.; Piner, R. D.; Stankovich, S.; Dikin, D. A.; Geisler, H.; Ventrice, C. A.; Ruoff, R. S., Reduction Kinetics of Graphene Oxide Determined by Electrical Transport Measurements and Temperature Programmed Desorption. *The Journal of Physical Chemistry C* **2009,** *113* (43), 18480-18486.
56. Koningsberger, D. C.; Oudenhuijzen, M. K.; De Graaf, J.; Van Bokhoven, J. A.; Ramaker, D. E., In situ X-ray absorption spectroscopy as a unique tool for obtaining information on hydrogen binding sites and electronic structure of supported Pt catalysts: towards an understanding of the compensation relation in alkane hydrogenolysis. *J. Catal.* **2003,** *216* (1-2), 178-191.
57. Pellegrini, R.; Leofanti, G.; Agostini, G.; Groppo, E.; Rivallan, M.; Lamberti, C., Pd-Supported Catalysts: Evolution of Support Porous Texture along Pd Deposition and Alkali-Metal Doping. *Langmuir* **2009,** *25* (11), 6476-6485.
58. Chu, P. M.; Guenther, F. R.; Rhoderick, G. C.; Lafferty, W. J., The NIST Quantitative Infrared Database. *J Res Natl Inst Stand Technol* **1999,** *104* (1), 59-81.
59. Chu, P. M.; Guenther, F. R.; Rhoderick, G. C.; Lafferty, W. J., Qunatitative Infrared Database. In *NIST Chemistry WebBook, NIST Standard Reference Database Number 69*, Linstrom, P. J.; Mallard, W. G., Eds. National Institute of Standards and Technology: Gaithersburg MD, Vol. 69.
60. Hall, P. J.; Calo, J. M., Secondary interactions upon thermal desorption of surface oxides from coal chars. *Energy & Fuels* **1989,** *3* (3), 370-376.

61. Schönherr, J.; Buchheim, J. R.; Scholz, P.; Adelhelm, P., Boehm Titration Revisited (Part I): Practical Aspects for Achieving a High Precision in Quantifying Oxygen-Containing Surface Groups on Carbon Materials. *C* **2018,** *4* (2).
62. Nordin, A., Chemical elemental characteristics of biomass fuels. *Biomass and Bioenergy* **1994,** *6* (5), 339-347.
63. Kohl, S.; Drochner, A.; Vogel, H., Quantification of oxygen surface groups on carbon materials via diffuse reflectance FT-IR spectroscopy and temperature programmed desorption. *Catalysis Today* **2010,** *150* (1), 67-70.
64. Haghseresht, F.; Lu, G. Q.; Whittaker, A. K., Carbon structure and porosity of carbonaceous adsorbents in relation to their adsorption properties. *Carbon* **1999,** *37* (9), 1491-1497.